Essential role for p38α mitogen-activated protein kinase in placental angiogenesis

John S. Mudgett*†‡, Jixiang Ding†§, Lucia Guh-Siesel*, Nicole A. Chartrain*, Lu Yang§, Shobhna Gopal*, and Michael M. Shen‡§

*Merck Research Laboratories, Rahway, NJ 07065; and §Center for Advanced Biotechnology and Medicine and Department of Pediatrics, University of Medicine and Dentistry of New Jersey–Robert Wood Johnson Medical School, 679 Hoes Lane, Piscataway, NJ 08854

Communicated by Aaron J. Shatkin, Center for Advanced Biotechnology and Medicine, Piscataway, NJ, July 10, 2000 (received for review June 2, 2000)

The p38 family of mitogen-activated protein kinases (MAPKs) mediates signaling in response to environmental stresses and inflammatory cytokines, but the requirements for the p38 MAPK pathway in normal mammalian development have not been elucidated. Here, we show that targeted disruption of the *p38α* MAPK gene results in homozygous embryonic lethality because of severe defects in placental development. Although chorioallantoic placentation is initiated appropriately in *p38α* null homozygotes, placental defects are manifest at 10.5 days postcoitum as nearly complete loss of the labyrinth layer and significant reduction of the spongiotrophoblast. In particular, *p38α* mutant placentas display lack of vascularization of the labyrinth layer as well as increased rates of apoptosis, consistent with a defect in placental angiogenesis. Furthermore, *p38α* mutants display abnormal angiogenesis in the embryo proper as well as in the visceral yolk sac. Thus, our results indicate a requirement for p38α MAPK in diploid trophoblast development and placental vascularization and suggest a more general role for p38 MAPK signaling in embryonic angiogenesis.

During mammalian embryogenesis, the development of the chorioallantoic placenta establishes the maternal–fetal interface, which facilitates oxygen and nutrient uptake by the fetal circulation (reviewed in ref. 1). A central feature of placental development is the formation of a complex vascular network within the labyrinth layer of the diploid trophoblast. This process of placental angiogenesis involves the rapid invasion of endothelial cells from the chorionic mesenchyme into the adjacent diploid trophoblast. Similarly, angiogenesis within the embryo and in the extraembryonic visceral yolk sac results in pruning and remodeling of a primitive capillary plexus to form a mature vascular network (reviewed in ref. 2).

In the present work, we show that placental as well as embryonic and yolk sac angiogenesis requires the activity of p38α mitogen-activated protein kinase (MAPK). Members of the mammalian p38 MAPK family were originally identified as mediators of responses to hyperosmolarity, as well as regulators of inflammatory cytokine synthesis (3–5). To date, four isoforms of the p38 MAPK family have been identified, which are encoded by distinct genetic loci (6–11). At least two of these family members (p38α and p38β) share several properties, including similar inhibition by p38 kinase inhibitors and overlap of upstream and downstream pathways (7, 12, 13), suggesting potential functional redundancies *in vivo*.

Although p38α MAPK was originally identified through its role in stress responses, we find that the p38α MAPK isoform also plays an essential role in normal embryonic development. We show through gene targeting that homozygosity for a null mutation in *p38α* results in embryonic lethality at midgestation stages, most likely as a consequence of defective placental development. In particular, we find that there are two distinct defects in the placenta, corresponding to a severe reduction in the spongiotrophoblast layer, as well as a near absence of the labyrinth layer because of the failure of vascularization by endothelial cells from the underlying chorionic plate. In addition, our observations of abnormal embryonic and yolk sac blood vessel organization suggest that p38α MAPK is not essential for early events in vasculogenesis, the process by which endothelial progenitors (angioblasts) differentiate to form a primary capillary plexus. Instead, p38α seems to be required for the vascular remodeling associated with angiogenesis.

Materials and Methods

Gene Targeting and Mouse Genotyping. Cosmid clones containing the mouse p38α gene were isolated from a 129SvEv genomic library. Targeted embryonic stem (ES) cell clones were obtained by using the AB2.1 and W9.5 ES lines, confirmed by Southern blot analysis with a unique upstream genomic probe, and injected into mouse blastocysts by using standard procedures. Chimeric mice were mated to C57BL/6J, BlkSw/J, Sw/J, and BALBc/J mice for generation of F_1 animals, which were interbred to generate litters for genotypic analysis. Genotyping was performed by Southern blotting or by PCR using genomic DNA prepared from tails or embryonic visceral yolk sac. Primers for genotyping were 5′-CCA ACC CCA GAA AGA AAT GA-3′ (forward primer for wild-type and targeted alleles); 5′-TGA GCC TGC AAA CAC AGA AG-3′ (reverse primer for wild-type allele); and 5′-TCC TGT AAG TCT GCA GAA ATT GAT-3′ (reverse primer for targeted allele).

Homozygous ES clones were obtained by culturing heterozygous ES cells in the presence of 1 mg/ml active G418, followed by screening of daughter colonies by Southern blot analysis (14). Protein was prepared from wild-type, heterozygous, and homozygous p38α ES cells and blotted with antibodies specific for the p38α protein (New England Biolabs) or antibodies that crossreact with multiple p38 isoforms (New England Biolabs, unpublished antiserum).

Histology, *in Situ* Hybridization, and Immunohistochemistry. Hematoxylin and eosin staining of sections from paraffin-embedded tissue was carried out by using standard methods. Methods for section *in situ* hybridization have been described (15). Immunohistochemistry and Western blotting for p38 isoforms were performed by using two polyclonal antisera, one that is specific for p38α and one that reacts with both p38α and p38β (New England Biolabs); immunohistochemical staining for platelet endothelial cell adhesion molecule (PECAM) was performed by using a monoclonal antibody (PharMingen) as described (16).

Abbreviations: MAPK, mitogen-activated protein kinase; dpc, days postcoitum; ES, embryonic stem; PECAM, platelet endothelial cell adhesion molecule; VEGF, vascular endothelial growth factor; TUNEL, terminal deoxynucleotidyltransferase-mediated UTP end labeling; kb, kilobase.

†J.S.M. and J.D. contributed equally to this work.

‡To whom reprint requests should be addressed. E-mail: john_mudgett@merck.com or mshen@cabm.rutgers.edu.

The publication costs of this article were defrayed in part by page charge payment. This article must therefore be hereby marked "*advertisement*" in accordance with 18 U.S.C. §1734 solely to indicate this fact.

Article published online before print: *Proc. Natl. Acad. Sci. USA*, 10.1073/pnas.180316397. Article and publication date are at www.pnas.org/cgi/doi/10.1073/pnas.180316397

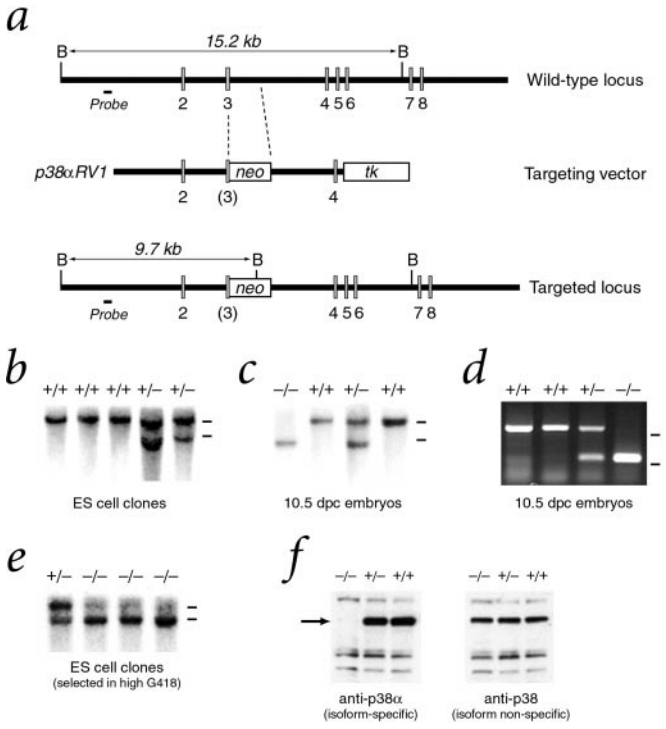

Fig. 1. Targeted disruption of the *p38α* gene. (*a*) The gene-targeting vector p38αRV1 inserts an antisense *PGK–neo* cassette into an *Eco*RI site in exon 3 and contains a 5′ flanking 4.5-kilobase (kb) *Eco*RI fragment and a 3′ flanking 3-kb *Sma*I–*Kpn*I fragment, resulting in deletion of the 3′ half of exon 3 and part of intron 3. (*b*) Southern blot analysis of ES cell clones with a unique 5′ genomic probe distinguishes a wild-type 15.2-kb *Bam*HI fragment from a 9.7-kb *Bam*HI fragment generated by the targeted allele. Bars at right indicate positions of 15-kb wild-type and 10-kb targeted alleles. (*c*) Southern analysis of genomic DNA digested with *Bam*HI from 10.5 dpc embryos obtained from a *p38α* heterozygous intercross. (*d*) PCR analysis of genomic DNA from visceral yolk sacs of 10.5 dpc embryos from a *p38α* heterozygous intercross. Bars at right indicate positions of markers at 500 and 250 bp. (*e*) Southern analysis of ES cell clones selected after growth in high concentrations (1 mg/ml) of G418 to obtain homozygosity for the *p38α* targeted allele. (*f*) Western analysis of total protein lysates from wild-type and targeted ES cells with antibodies that are specific for p38α or that crossreact with multiple p38 MAPK isoforms.

Terminal deoxynucleotidyltransferase-mediated UTP end labeling (TUNEL) analysis was performed as described (17).

Results

Generation of *p38α*-Deficient ES Cells and Mice. To determine the biological function of the p38α isoform, we created a null allele by targeted gene disruption (Fig. 1 *a* and *b*). Heterozygous *p38α* mice appeared normal and fertile, whereas no homozygous mutants were recovered at birth (Table 1). To confirm that the null phenotype did not depend on ES cell line or strain background, we targeted the *p38α* gene in two different ES cell lines (AB2.1 and W9.5) and crossed the resulting progeny into four different strain backgrounds (outbred Black Swiss and inbred 129/SvEv, C57BL/6, and BALB/c), obtaining similar phenotypes in each case. Genotypic analysis of embryonic litters in a 129/SvEv-C57BL/6 hybrid background revealed that *p38α* null homozygotes could be recovered at the expected Mendelian ratios until 10.5 days postcoitum (dpc), with most homozygous mutants dying *in utero* between 10.5 and 12.5 dpc (Fig. 1 *c* and *d*, and Table 1).

To investigate cellular viability of the *p38α* null, we generated homozygous mutant ES cells by selection in high concentrations of G418 (Fig. 1*e*) (14). By Western blot analysis of ES cells with a polyclonal antiserum specific for p38α (Fig. 1*f*), we found that homozygous mutant ES cells lacked p38α protein, confirming that the targeted mutation generates a functionally null allele. Western analysis with a control antibody that crossreacts with multiple p38 isoforms confirmed expression of other p38 isoforms in the *p38α* null cells (Fig. 1*f*). The p38α-deficient ES cells displayed no overt growth or differentiation phenotypes in early embryoid body culture, as judged by their morphology; however, attempts to culture primary fibroblasts from *p38α* null embryos were unsuccessful because of cellular inviability after the first passage (data not shown).

Table 1. Genotype analysis of progeny from *p38α* heterozygous intercrosses

	Genotype		
Age	Wild type	Heterozygous	Homozygous mutant
8.5 dpc	4	4	2
9.5 dpc	14	16	7
10.5 dpc	28	69	25 (1/25 inviable)
11.5 dpc	17	31	9 (8/9 inviable)
12.5 dpc	11	16	8 (6/8 inviable)
13.5 dpc	6	14	5 (4/5 inviable)
15.5–16.5 dpc	6	6	3 (3/3 inviable)
Postnatal (129Sv × C57B1/6)	117	204	0
Postnatal (129Sv × BlkSw)	18	15	0
Postnatal (129Sv × Sw)	22	17	0
Postnatal (129Sv × BALB/c)	21	10	0

Genotyped embryos that were severely retarded or in the process of resorbing were scored as inviable. Embryonic analyses were performed with 129Sv × C57B1/6 F_2 embryos. Postnatal mice were scored at 3 wk of age.

Expression of *p38α* in Diploid Trophoblast. Immunohistochemical analysis of *p38α* expression during wild-type embryogenesis with the α-isoform-specific antibody revealed that protein levels were low but uniform in embryos at 9.5 dpc, whereas they were relatively high in the diploid trophoblast of the placenta, including the labyrinth layer (Fig. 2*a*). The specificity of the polyclonal antisera was further demonstrated by parallel immunohistochemical analysis of homozygous *p38α* mutant placentas, which showed absence of staining (Fig. 2*b*). In contrast, equivalent levels of staining were detected in the maternal decidual tissue surrounding both wild-type and homozygous mutant placentas (Fig. 2 *a* and *b*). These data demonstrate that *p38α* expression is abundant in the tissues that are severely affected in targeted mutants, as described below.

Placental Defects in *p38α*-Deficient Mouse Embryos. To determine the basis for the embryonic lethality of *p38α* mutants, we examined the morphology and histology of embryos and extraembryonic tissues at 9.5–11.5 dpc. Although *p38α* mutant embryos were often developmentally retarded and smaller than their wild-type littermates by 11.5 dpc (Fig. 3*a*), we observed no consistent overt defects that might result in embryonic lethality, such as gross abnormalities in primitive hematopoiesis or cardiac development (data not shown). In contrast, the placenta appeared morphologically thinner in the homozygous mutants at 10.5 dpc and was frequently paler in color, suggesting a defect in vascularization (Fig. 3 *b* and *c*). Although formation of the chorioallantoic connection appeared normal, histological analyses of the placentas at 10.5 dpc revealed a highly abnormal morphology of the diploid trophoblast, with a loss of the labyrinth layer and a greatly reduced spongiotrophoblast (Fig. 3 *d–g*). By 11.5 dpc, *p38α* mutants displayed a severely decreased vascular network within the labyrinth layer, as shown by a nearly

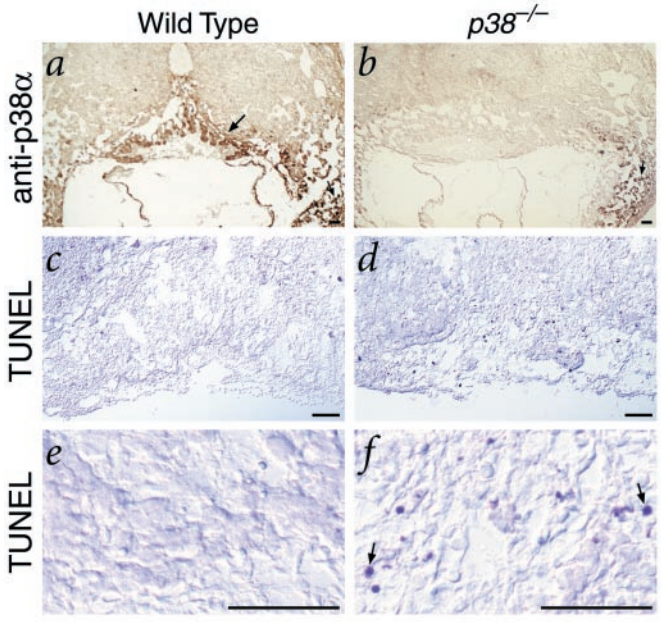

Fig. 2. Expression of p38α MAPK and detection of apoptosis in wild-type and *p38α* mutant placentas. (*a* and *b*) Immunohistochemical detection of p38α in placenta and maternal decidua. Note the strong staining in the wild-type diploid trophoblast (arrows) in the wild type (*a*), but not the mutant (*b*); in contrast, staining in the maternal decidual cells is unaffected (arrowheads). (*c–f*) TUNEL analysis of wild-type and *p38α* mutant placentas shows nearly complete lack of apoptotic cells in the diploid trophoblast of the wild-type placenta (*c* and *e*), but abundant labeled cells in the mutant trophoblast (*d* and *f*). (Scale bars represent 100 μm.)

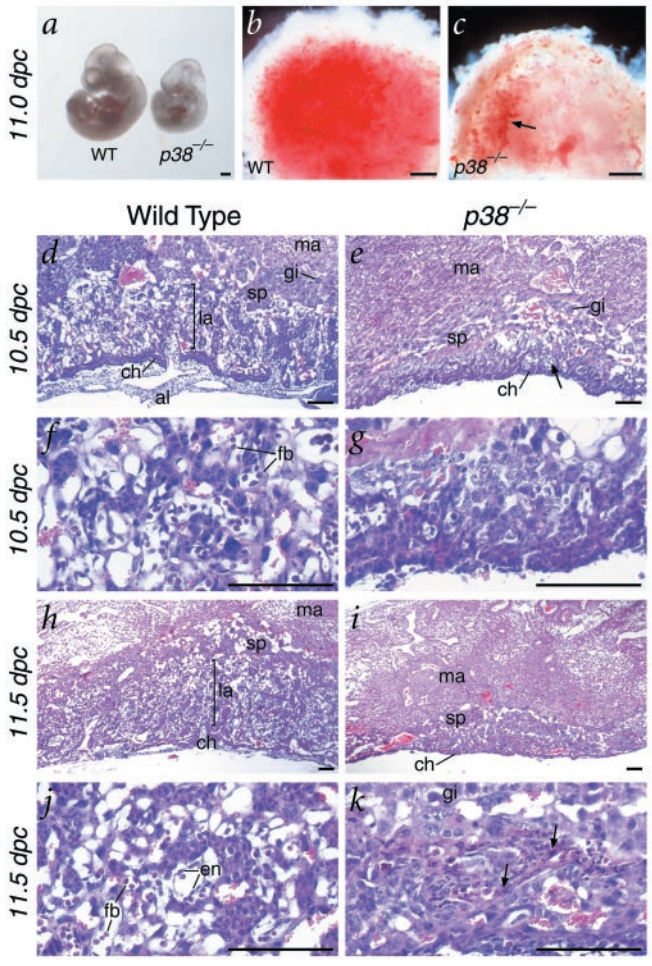

Fig. 3. Morphology and histology of wild-type and *p38α* mutant embryos and placentas. (*a*) Gross morphology of a wild-type and *p38α* mutant littermate at 11.0 dpc, showing developmental retardation of the homozygote. (*b* and *c*) Ventral view of the placentas of a wild-type and *p38α* mutant, showing apparent decreased vascularization of the mutant placenta, as shown by its paler red color (arrow in *c*). (*d–k*) Hematoxylin and eosin-stained sections of placentas from wild-type (*d*, *f*, *h*, and *j*) and *p38α* homozygous mutant littermates (*e*, *g*, *i*, and *k*). (*d* and *e*) At 10.5 dpc, the developing labyrinth and spongiotrophoblast layers found in the wild type (*d*) are significantly decreased in thickness in the *p38α* mutant (*e*, arrow). (*f* and *g*) High-power views show a nearly complete lack of circulating fetal blood cells in the mutant. (*h* and *i*) By 11.5 dpc, the labyrinth layer is essentially missing and the spongiotrophoblast layer is greatly diminished in the *p38α* mutant compared with wild-type. (*j* and *k*) High-power views show that the placental vasculature with differentiated endothelial cells and circulating fetal blood cells (*j*) is nearly completely abolished in the *p38α* mutant, which instead contains apparent necrotic regions (*k*, arrows). (Scale bars in *a–c* represent 0.5 mm; bars in *d–k* represent 100 μm.) Abbreviations: al, allantois; ch, chorionic plate; en, endothelial cells; fb, fetal blood cells; gi, trophoblast giant cells; la, labyrinthine trophoblast; ma, maternal decidual tissue; sp, spongiotrophoblast; WT, wild type.

complete absence of blood vessels lined with endothelial cells (Fig. 3 *h–k*). This failure to establish the maternal–fetal interface for oxygen and nutrient exchange is likely to account for the midgestation embryonic lethality of *p38α* mutants.

To confirm the nature of the placental defect in *p38α* mutants, we examined the expression of several markers for the various layers of the developing placenta at 9.5 and 10.5 dpc. Using *in situ* hybridization, we examined the expression of the basic helix–loop–helix gene *eHAND*, which marks both diploid trophoblast and trophoblast giant cells (18, 19), and *MASH2*, which marks diploid trophoblast cells of the spongiotrophoblast and labyrinth layers (20), and observed that the staining in *p38α* mutants was reduced in a manner that corresponded to the decrease in placental size (Fig. 4 *a–d*). To analyze the distribution of trophoblast giant cells, we examined the expression of its specific markers proliferin (*PLF-1*; ref. 21) and placental lactogen-I (*MPL-1*; ref. 22) and found that there were no apparent abnormalities in this cell population (Fig. 4 *e–h*). In contrast, there was a significant reduction in the spongiotrophoblast layer, as determined by expression of *4311* (23) and the tyrosine kinase receptor *FLT-1* (refs. 24 and 25; Fig. 4 *i–l*). Most strikingly, expression of the homeobox gene *Esx1*, which marks the chorionic plate and labyrinth layer (26, 27), was essentially normal at 9.5 dpc but was almost completely lost at 10.5 dpc (Fig. 4 *m–p*), supporting the histological evidence for a severe defect in the labyrinth layer.

Defective Placental and Embryonic Angiogenesis in *p38α* Mutants. To examine the development of the placental vascular network, we used a monoclonal antibody against PECAM, a marker for endothelial cells. Immunohistochemical staining revealed a relatively normal distribution of angiogenic mesenchyme in the chorionic plate of *p38α* mutants at 9.5 dpc (Fig. 4 *q* and *r*). During wild-type placentation, this angiogenic mesenchyme rapidly infiltrates the developing labyrinth layer, forming a dense vasculature containing circulating fetal blood cells (Fig. 3 *f* and *j* and Fig. 4*s*). However, in *p38α* mutants at 10.5 dpc, there was a clear defect in this invasion process, as shown by the paucity of anti-PECAM staining of endothelial cells in the greatly reduced labyrinth layer, despite abundant staining in the chorionic plate (Fig. 3 *g* and *k* and Fig. 4*t*).

Consistent with this vascularization defect, we observed a

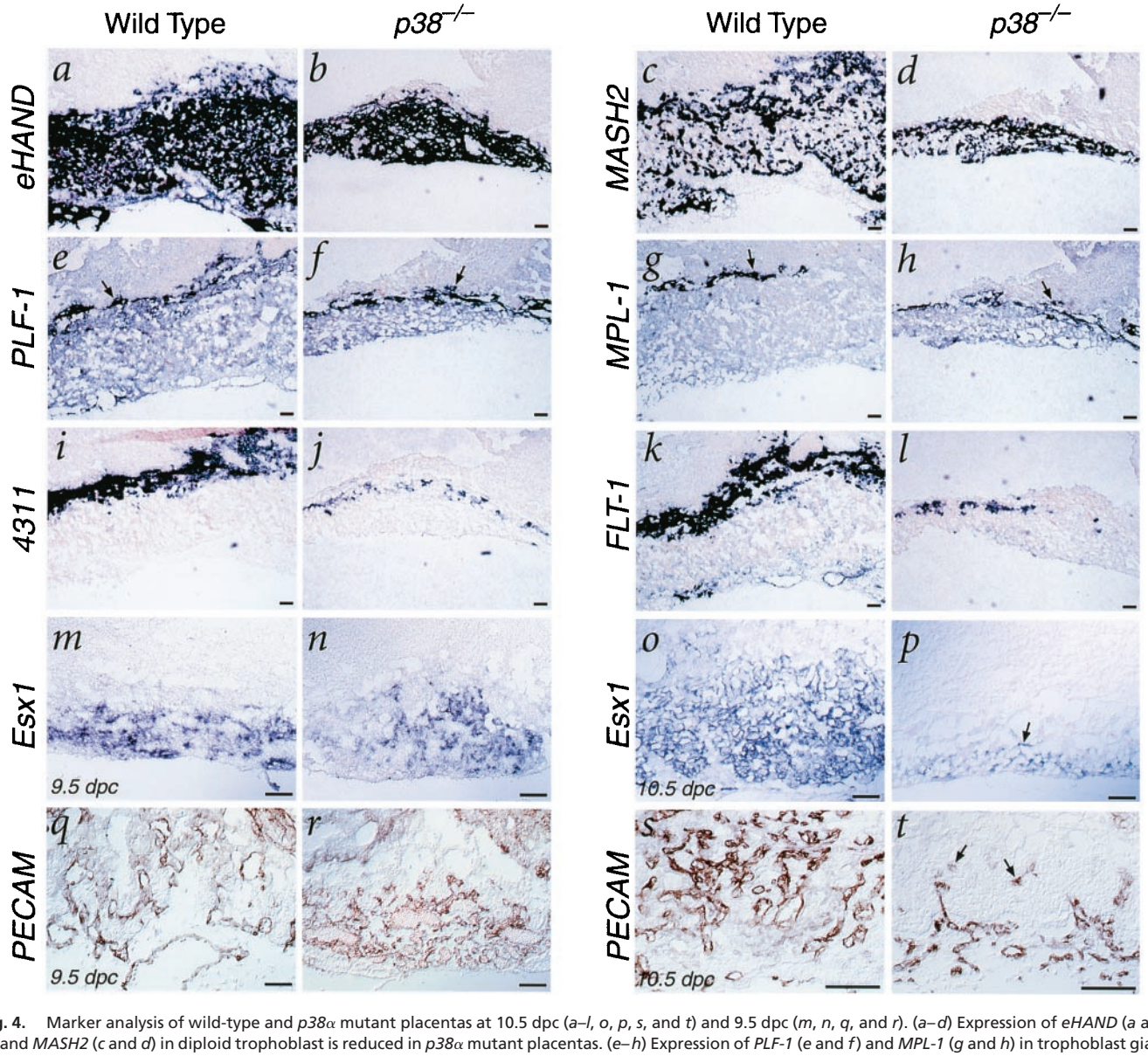

Fig. 4. Marker analysis of wild-type and *p38α* mutant placentas at 10.5 dpc (*a–l*, *o*, *p*, *s*, and *t*) and 9.5 dpc (*m*, *n*, *q*, and *r*). (*a–d*) Expression of *eHAND* (*a* and *b*) and *MASH2* (*c* and *d*) in diploid trophoblast is reduced in *p38α* mutant placentas. (*e–h*) Expression of *PLF-1* (*e* and *f*) and *MPL-1* (*g* and *h*) in trophoblast giant cells (arrows) is unaffected in *p38α* mutants. (*i–l*) Expression of *4311* and *FLT-1* in spongiotrophoblast is greatly reduced in *p38α* mutant placentas. (*m–p*) At 9.5 dpc, expression of *Esx1* in the chorionic plate and labyrinth layer is relatively normal in *p38α* mutants (*n*) relative to wild type (*m*), whereas by 10.5 dpc, the expression of *Esx1* is greatly diminished (*p*, arrow). (*q–t*) Immunohistochemical staining for PECAM marks endothelial cells in the allantoic plate and developing labyrinth at 9.5 dpc in both wild-type (*q*) and *p38α* mutant placentas (*r*). At 10.5 dpc, infiltration of endothelial cells into the labyrinth layer is well-advanced in the wild-type placenta (*s*), but only a few PECAM-positive regions can be detected in the labyrinth layer of the *p38α* mutant (*t*, arrows). (Scale bars represent 100 μm.)

significantly greater number of dying cells in the labyrinth layer of mutant placentas at 10.5 dpc, as determined by TUNEL analysis; in contrast, no differences were observed in the trophoblast giant cell population (Fig. 2 *c–f*). This increase in apoptosis may represent a primary defect in *p38α* mutant mice that is unrelated to the angiogenesis defect or may be secondary to the failure of placental vascularization.

Finally, we found that angiogenic defects existed in other *p38α* mutant tissues by using whole-mount immunohistochemistry with an anti-PECAM antibody. Thus, in the developing brain of wild-type littermate embryos at 10.5 dpc, angiogenic pruning and remodeling of the vascular plexus had already resulted in an intricate network of larger vessels and minor branches (Fig. 5*a*). In contrast, *p38α* mutant embryos displayed numerous vessels of roughly similar size that were not organized in a branching vascular tree (Fig. 5*b*). Similarly, wild-type visceral yolk sacs at 10.5 dpc displayed a well organized vascular network as a result of angiogenic remodeling, whereas *p38α* mutant visceral yolk sacs lacked major blood vessels and instead retained a primitive capillary plexus (Fig. 5 *c* and *d*). These results suggest that vasculogenesis is largely unaffected in *p38α* mutant embryos and visceral yolk sacs, whereas there is an angiogenic defect in embryonic and extraembryonic tissues that correlates with the defect in placental vascularization.

Discussion

Essential Role for p38α MAPK in Placental Angiogenesis and Trophoblast Development. Although numerous studies have suggested essential requirements for p38 MAPKs in inflammatory and environmental stress responses, the roles of the p38 MAPK

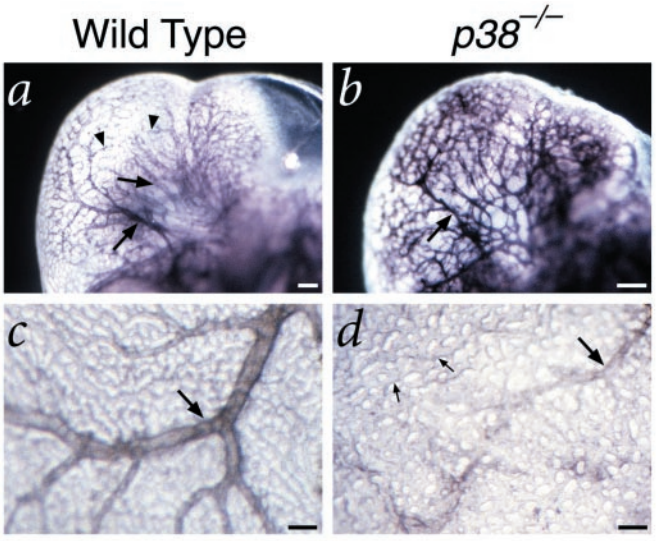

Fig. 5. PECAM whole-mount immunohistochemistry of embryos and visceral yolk sacs at 10.5 dpc. (*a* and *b*) Vasculature of the developing brain in a wild-type littermate (*a*) and *p38α* mutant embryo (*b*). Note that the tree-like architecture of the major vessels (arrows) connecting to minor branches (arrowheads) in the wild-type differs significantly from the relatively uniform size and disorganized pattern of the vasculature in the mutant embryo. (*c* and *d*) Vasculature of the visceral yolk sac in a wild-type littermate (*c*) and *p38α* mutant embryo (*d*). Although the wild-type yolk sac displays major vessels (arrows) and branches, the mutant yolk sac has relatively few major vessels with abnormal morphology (arrow), and retains a primitive capillary plexus (small arrows).

pathway and of specific p38 isoforms in normal development have been unclear. Recent evidence supporting a central role for p38 MAPK function in embryogenesis has been provided through analysis of the *Drosophila* p38 MAPK pathway (28). Our present analysis of *p38α* mutants indicates that p38α MAPK has a previously unsuspected role in placental and embryonic angiogenesis in mammalian development.

To some extent, the defect in placental vascularization in *p38α* mutants resembles the defects previously described for targeted mutations of the helix–loop–helix gene *Tfeb* (29), the transcription factor GCMa (30), and the von Hippel–Lindau tumor suppressor gene *VHL* (31). In addition, several other mutants are known to result in complete or nearly complete loss of the labyrinth layer, including targeted mutants for the signaling factor *HGF* (32), the homeobox gene *Dlx3* (33), and the chaperonin *HSP90*A (34). However, the potential regulatory relationships, if any, between *p38α* and these other genes in the pathways for placental angiogenesis remains to be examined. Notably, none of these other mutants have been reported to have defects in embryonic or visceral yolk sac angiogenesis.

In addition to angiogenesis defects, *p38α* mutants display a significant reduction in the spongiotrophoblast layer, suggesting an independent requirement for *p38α* in diploid trophoblast development. Such a role may be supported by the observation that p38 MAPK is activated in cultured human syncytiotrophoblast in response to placental growth factor (PlGF), which is related to vascular endothelial growth factor (VEGF; ref. 35). Moreover, PlGF signaling has also been shown to inhibit apoptosis in response to growth factor deprivation (35), which may be consistent with the elevated rate of trophoblast apoptosis seen in *p38α* mutant placentas.

Our analysis of *p38α* mutant mice is complementary to recent observations of Allen *et al.* (36) on the phenotype of p38α-deficient ES cells. These workers found that p38α-deficient ES cells displayed greatly reduced activation of MAPKAP kinase 2 in response to chemical stress inducers such as anisomycin or sodium arsenite (36). Moreover, p38α-deficient ES cell-derived embryoid bodies displayed a significantly impaired response to the cytokine IL-1 (36), supporting the previously proposed role for p38 MAPK in inflammatory responses.

Regulatory Relationships with Other Members of MAPK Signaling Pathways. Recent work has shown that loss of function for several other members of MAPK signaling pathways also leads to embryonic lethality (e.g., refs. 37 and 38). In particular, mutants for the MAPK kinase kinase Mekk3 also display angiogenic defects in both the placental labyrinth layer and in embryos (39), consistent with a role for Mekk3 in the signaling pathway upstream of p38 MAPK (40). Conversely, the MEF2C transcription factor is believed to represent a primary downstream target of p38 MAPK activity (41, 42), consistent with the placental vascularization phenotypes observed in MEF2C mutants (43, 44). Thus, our findings provide support for a signaling pathway in which Mekk3 activity leads to the activation of p38 MAPK, which in turn regulates MEF2C.

However, less consistent with this model is the finding that mice deficient for *Mkk3* are viable with defects in IL-12 production (45), perhaps because of functional redundancy of Mkk3 with other MAPK kinases that regulate p38 MAPK, such as Mkk6. Moreover, *Mek1* mutant mice also display a relatively less severe placental vascularization defect (46), although p38α is unlikely to be regulated by Mek1. Taken together, these results suggest that placental angiogenesis is regulated by independent MAPK pathways.

Potential Functions of p38α MAPK Signaling in Angiogenesis. Our observations raise the possibility that p38α MAPK activity is required for the angiogenic response to the hypoxic environment found during early chorioallantoic placentation. Hypoxia induces a physiological response mediated by a heterodimer of the basic helix–loop–helix factors HIF-1α and HIF-1β (also known as ARNT), which is known to induce expression of VEGF (47–49). Notably, loss of function of HIF-1β results in severe defects in placental vascularization (50).

Two distinct potential roles can be envisaged for p38 MAPK activity in the hypoxia response pathway. One possible model is that p38 MAPK activation represents a downstream event in signaling by VEGF and/or other angiogenic factors and their receptors. In support of this model, p38 MAPK activity has been shown to be required for cell migration by cultured human umbilical vein endothelial cells in response to VEGF (51), perhaps consistent with the defects in labyrinth invasion by allantoic angiogenic mesenchyme in *p38α* mutants. An alternative possibility is that hypoxia might activate p38 MAPK, which might indirectly facilitate expression of angiogenic factors such as VEGF; consistent with this view, the p38α and p38γ isoforms are specifically activated in PC12 cells in response to hypoxic conditions (52). Further investigation should elucidate the specific function of p38α MAPK in placental angiogenesis.

Note Added in Proof. While this manuscript was in press, two other papers describing the phenotype of p38α knockout mice were published (53, 54); also see commentary by J. Ihle (55).

We thank Nishita Desai, Sandy Price, and Qin Xu for technical assistance, Mengqing Xiang for advice on TUNEL assays, Jay Cross, Dan Linzer, and Janet Rossant for generous gifts of probes, and New England Biolabs for the gift of antibodies. We are particularly grateful to Michael Tocci for initiating this collaboration, and to Cory Abate-Shen and Yu-Ting Yan for helpful discussions and comments on the manuscript. This work was supported by a postdoctoral fellowship from the American Heart Association, New Jersey Affiliate (to J.D.) and by Grants HL60212 and HD38766 from the National Institutes of Health (to M.M.S).

1. Cross, J. C., Werb, Z. & Fisher, S. J. (1994) *Science* **266,** 1508–1518.
2. Risau, W. (1997) *Nature (London)* **386,** 671–674.
3. Han, J., Lee, J. D., Bibbs, L. & Ulevitch, R. J. (1994) *Science* **265,** 808–811.
4. Rouse, J., Cohen, P., Trigon, S., Morange, M., Alonso-Llamazares, A., Zamanillo, D., Hunt, T. & Nebreda, A. R. (1994) *Cell* **78,** 1027–1037.
5. Lee, J. C., Laydon, J. T., McDonnell, P. C., Gallagher, T. F., Kumar, S., Green, D., McNulty, D., Blumenthal, M. J., Heys, J. R., Landvatter, S. W., *et al.* (1994) *Nature (London)* **372,** 739–746.
6. Li, Z., Jiang, Y., Ulevitch, R. J. & Han, J. (1996) *Biochem. Biophys. Res. Commun.* **228,** 334–340.
7. Jiang, Y., Chen, C., Li, Z., Guo, W., Gegner, J. A., Lin, S. & Han, J. (1996) *J. Biol. Chem.* **271,** 17920–17926.
8. Lechner, C., Zahalka, M. A., Giot, J. F., Moller, N. P. & Ullrich, A. (1996) *Proc. Natl. Acad. Sci. USA* **93,** 4355–4359.
9. Jiang, Y., Gram, H., Zhao, M., New, L., Gu, J., Feng, L., Di Padova, F., Ulevitch, R. J. & Han, J. (1997) *J. Biol. Chem.* **272,** 30122–30128.
10. Wang, X. S., Diener, K., Manthey, C. L., Wang, S., Rosenzweig, B., Bray, J., Delaney, J., Cole, C. N., Chan-Hui, P. Y., Mantlo, N., *et al.* (1997) *J. Biol. Chem.* **272,** 23668–23674.
11. Cuenda, A., Cohen, P., Buee-Scherrer, V. & Goedert, M. (1997) *EMBO J.* **16,** 295–305.
12. Enslen, H., Raingeaud, J. & Davis, R. J. (1998) *J. Biol. Chem.* **273,** 1741–1748.
13. New, L., Jiang, Y., Zhao, M., Liu, K., Zhu, W., Flood, L. J., Kato, Y., Parry, G. C. & Han, J. (1998) *EMBO J.* **17,** 3372–3384.
14. Mortensen, R. M., Conner, D. A., Chao, S., Geisterfer-Lowrance, A. A. & Seidman, J. G. (1992) *Mol. Cell. Biol.* **12,** 2391–2395.
15. Sciavolino, P. J., Abrams, E. W., Yang, L., Austenberg, L. P., Shen, M. M. & Abate-Shen, C. (1997) *Dev. Dyn.* **209,** 127–138.
16. Wang, H. U., Chen, Z. F. & Anderson, D. J. (1998) *Cell* **93,** 741–753.
17. Xiang, M., Gao, W. Q., Hasson, T. & Shin, J. J. (1998) *Development (Cambridge, U.K.)* **125,** 3935–3946.
18. Cross, J. C., Flannery, M. L., Blanar, M. A., Steingrimsson, E., Jenkins, N. A., Copeland, N. G., Rutter, W. J. & Werb, Z. (1995) *Development (Cambridge, U.K.)* **121,** 2513–2523.
19. Cserjesi, P., Brown, D., Lyons, G. E. & Olson, E. N. (1995) *Dev. Biol.* **170,** 664–678.
20. Guillemot, F., Caspary, T., Tilghman, S. M., Copeland, N. G., Gilbert, D. J., Jenkins, N. A., Anderson, D. J., Joyner, A. L., Rossant, J. & Nagy, A. (1995) *Nat. Genet.* **9,** 235–242.
21. Lee, S. J., Talamantes, F., Wilder, E., Linzer, D. I. & Nathans, D. (1988) *Endocrinology* **122,** 1761–1768.
22. Faria, T. N., Ogren, L., Talamantes, F., Linzer, D. I. & Soares, M. J. (1991) *Biol. Reprod.* **44,** 327–331.
23. Lescisin, K. R., Varmuza, S. & Rossant, J. (1988) *Genes Dev.* **2,** 1639–1646.
24. Dumont, D. J., Fong, G. H., Puri, M. C., Gradwohl, G., Alitalo, K. & Breitman, M. L. (1995) *Dev. Dyn.* **203,** 80–92.
25. Yamaguchi, T. P., Dumont, D. J., Conlon, R. A., Breitman, M. L. & Rossant, J. (1993) *Development (Cambridge, U.K.)* **118,** 489–498.
26. Li, Y., Lemaire, P. & Behringer, R. R. (1997) *Dev. Biol.* **188,** 85–95.
27. Yan, Y.-T., Stein, S. M., Ding, J., Shen, M. M. & Abate-Shen, C. (2000) *Mol. Cell. Biol.* **20,** 661–671.
28. Suzanne, M., Irie, K., Glise, B., Agnes, F., Mori, E., Matsumoto, K. & Noselli, S. (1999) *Genes Dev.* **13,** 1464–1474.
29. Steingrimsson, E., Tessarollo, L., Reid, S. W., Jenkins, N. A. & Copeland, N. G. (1998) *Development (Cambridge, U.K.)* **125,** 4607–4616.
30. Schreiber, J., Riethmacher-Sonnenberg, E., Riethmacher, D., Tuerk, E. E., Enderich, J., Bosl, M. R. & Wegner, M. (2000) *Mol. Cell. Biol.* **20,** 2466–2474.
31. Gnarra, J. R., Ward, J. M., Porter, F. D., Wagner, J. R., Devor, D. E., Grinberg, A., Emmert-Buck, M. R., Westphal, H., Klausner, R. D. & Linehan, W. M. (1997) *Proc. Natl. Acad. Sci. USA* **94,** 9102–9107.
32. Uehara, Y., Minowa, O., Mori, C., Shiota, K., Kuno, J., Noda, T. & Kitamura, N. (1995) *Nature (London)* **373,** 702–705.
33. Morasso, M. I., Grinberg, A., Robinson, G., Sargent, T. D. & Mahon, K. A. (1999) *Proc. Natl. Acad. Sci. USA* **96,** 162–167.
34. Voss, A. K., Thomas, T. & Gruss, P. (2000) *Development (Cambridge, U.K.)* **127,** 1–11.
35. Desai, J., Holt-Shore, V., Torry, R. J., Caudle, M. R. & Torry, D. S. (1999) *Biol. Reprod.* **60,** 887–892.
36. Allen, M., Svensson, L., Roach, M., Hambor, J., McNeish, J. & Gabel, C. A. (2000) *J. Exp. Med.* **191,** 859–870.
37. Sabapathy, K., Jochum, W., Hochedlinger, K., Chang, L., Karin, M. & Wagner, E. F. (1999) *Mech. Dev.* **89,** 115–124.
38. Yang, D., Tournier, C., Wysk, M., Lu, H. T., Xu, J., Davis, R. J. & Flavell, R. A. (1997) *Proc. Natl. Acad. Sci. USA* **94,** 3004–3009.
39. Yang, J., Boerm, M., McCarty, M., Bucana, C., Fidler, I. J., Zhuang, Y. & Su, B. (2000) *Nat. Genet.* **24,** 309–313.
40. Deacon, K. & Blank, J. L. (1999) *J. Biol. Chem.* **274,** 16604–16610.
41. Han, J., Jiang, Y., Li, Z., Kravchenko, V. V. & Ulevitch, R. J. (1997) *Nature (London)* **386,** 296–299.
42. Yang, S. H., Galanis, A. & Sharrocks, A. D. (1999) *Mol. Cell. Biol.* **19,** 4028–4038.
43. Lin, Q., Lu, J., Yanagisawa, H., Webb, R., Lyons, G. E., Richardson, J. A. & Olson, E. N. (1998) *Development (Cambridge, U.K.)* **125,** 4565–4574.
44. Bi, W., Drake, C. J. & Schwarz, J. J. (1999) *Dev. Biol.* **211,** 255–267.
45. Lu, H.-T., Yang, D. D., Wysk, M., Gatti, E., Mellman, I., Davis, R. J. & Flavell, R. A. (1999) *EMBO J.* **18,** 1845–1857.
46. Giroux, S., Tremblay, M., Bernard, D., Cadrin-Girard, J.-F., Aubry, S., Larouche, L., Rousseau, S., Huot, J., Landry, J., Jeannotte, L. & Charron, J. (1999) *Curr. Biol.* **9,** 369–372.
47. Forsythe, J. A., Jiang, B. H., Iyer, N. V., Agani, F., Leung, S. W., Koos, R. D. & Semenza, G. L. (1996) *Mol. Cell. Biol.* **16,** 4604–4613.
48. Arany, Z., Huang, L. E., Eckner, R., Bhattacharya, S., Jiang, C., Goldberg, M. A., Bunn, H. F. & Livingston, D. M. (1996) *Proc. Natl. Acad. Sci. USA* **93,** 12969–12973.
49. Iyer, N. V., Kotch, L. E., Agani, F., Leung, S. W., Laughner, E., Wenger, R. H., Gassmann, M., Gearhart, J. D., Lawler, A. M., Yu, A. Y. & Semenza, G. L. (1998) *Genes Dev.* **12,** 149–162.
50. Kozak, K. R., Abbott, B. & Hankinson, O. (1997) *Dev. Biol.* **191,** 297–305.
51. Rousseau, S., Houle, F., Landry, J. & Huot, J. (1997) *Oncogene* **15,** 2169–2177.
52. Conrad, P. W., Rust, R. T., Han, J., Millhorn, D. E. & Beitner-Johnson, D. (1999) *J. Biol. Chem.* **274,** 23570–23576.
53. Tamura, K., Sudo, T., Senftleben, U., Dadak, A. M., Johnson, R. & Karin, M. (2000) *Cell* **102,** 221–231.
54. Adams, R. H., Porras, A., Alonso, G., Jones, M., Vintersten, K., Panelli, S., Valladares, A., Perez, L., Klein, R. & Nebreda, A. R. (2000) *Mol. Cell* **6,** 109–116.
55. Ihle, J. (2000) *Cell* **102,** 131–134.